RSC Advances

RSCPublishing

PAPER

View Article Online
View Journal | View Issue

Cite this: *RSC Advances*, 2013, **3**, 16802

A highly selective and ratiometric fluorescent sensor for relay recognition of zinc(II) and sulfide ions based on modulation of excited-state intramolecular proton transfer†

Lijun Tang,* Mingjun Cai, Pei Zhou, Jia Zhao, Keli Zhong, Shuhua Hou and Yanjiang Bian

Received 13th June 2013,
Accepted 12th July 2013

DOI: 10.1039/c3ra42931h

www.rsc.org/advances

A new fluorescent 2-(2′-aminophenyl)benzimidazole derivatized sensor **BMD** was designed and synthesized. In CH_3CN/H_2O (2 : 8, v/v, HEPES 10 mM, pH 7.4) solution, sensor **BMD** displays two emission bands and exhibits a highly selective and ratiometric response to Zn^{2+} ions with a distinctly longer-wavelength emission blue shifted through the inhibition of the excited-state intramolecular proton transfer (ESIPT) process. **BMD** can clearly discriminate Zn^{2+} from Cd^{2+} and other metal ions. Moreover, the *in situ* generated **BMD**-Zn^{2+} solution exhibits a highly selective and ratiometric response to S^{2-} among various anions and thiol-containing amino acids *via* Zn^{2+} displacement approach, which results in a revival of the ESIPT phenomenon of free **BMD**. These results demonstrate that **BMD** can serve as a ratiometric sensor for sequential recognition of Zn^{2+} and S^{2-} in aqueous solution through inhibition and turn-on of ESIPT process.

1. Introduction

The development of chemical probes for highly selective recognition of biologically and environmentally important heavy and transition metal (HTM) ions as well as anions has received increasing attention due to the important roles they play in chemical, biological and environmental processes.[1] As the second most abundant transition metal ion in human body, Zn^{2+} plays critical roles in a variety of biological processes, such as gene transcription, signal transmission, and mammalian reproduction.[2] The normal Zn^{2+} content of blood plasma is 12 to 16 μM in humans,[2d] however, disruption of Zn^{2+} concentration in cells can result in some pathological processes including Alzheimer's disease, epilepsy and infantile diarrhoea.[2c,3] In recent years, considerable efforts have been focused on the development of fluorescent probes for Zn^{2+} due to the high sensitivity and easy operability of fluorescence techniques.[4]

Fluorescent probes that exhibit a ratiometric response to Zn^{2+} are more attractive and are still highly desired. This kind of probe can eliminate the effects of some factors such as emission collection efficiency, the environment around the sensor, sensor concentration, bleaching and illumination intensity.[5] On the other hand, Zn^{2+} recognition often suffers from the interference of Cd^{2+},[6] because these two metals are in the same main group in the Periodic Table and have very similar chemical properties. Although many successful fluorescent probes for Zn^{2+} and Cd^{2+} have been reported,[7] the design of single fluorescent probes that can successfully discriminate Zn^{2+} from Cd^{2+} still remains attractive and challenging.[8]

Sulfide, as a toxic traditional pollutant, has received increasing attention. Although sulfide has many applicable utilities in the fields of manufacturing of sulfuric acid, dyes and cosmetics,[9] exposure to high levels of sulfide can lead to various physiological and biochemical problems including irritation in mucous membranes, unconsciousness, and respiratory paralysis.[9,10] Therefore, sulfide detection has received immense interest and a number of S^{2-} ion-selective fluorescent probes have been developed.[11] Sulfide sensing by using a metal complex *via* S^{2-}-induced metal ion displacement has been proved to be an effective method.[11b–f,12] However, fluorescent sulfide detection with a Zn^{2+} complex is still rare.

Herein we report the synthesis and ion recognition behavior of a new di(2-picolyl)amine (DPA) decorated benzimidazole derivative (**BMD**) (Fig. 1). **BMD** can discriminate Zn^{2+} from Cd^{2+} and other metal ions through distinct fluorescence responses; the *in situ* generated **BMD**-Zn^{2+} complex exhibits

---

Department of Chemistry, Liaoning Provincial Key Laboratory for the Synthesis and Application of Functional Compounds, Bohai University, Jinzhou, China. E-mail: ljtang@bhu.edu.cn; Fax: +86 416 3400158; Tel: +86 416 3400302

† Electronic supplementary information (ESI) available: Cif file, ^1H NMR, ^{13}C NMR and HRMS of sensor BMD, and other supplementary data. CCDC 919147. For ESI and crystallographic data in CIF or other electronic format see DOI: 10.1039/c3ra42931h

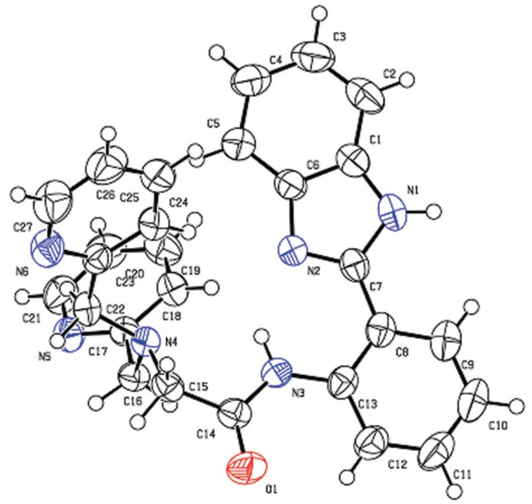

Fig. 1 Molecular structure of sensor **BMD** with the atomic numbering scheme. The solvent molecule (H_2O) was omitted for clarity.

highly selective ratiometric recognition to S^{2-} *via* a Zn^{2+} displacement approach. As far as we are aware, this is the first example for ratiometric fluorescent recognition of Zn^{2+} and S^{2-} with a simple Zn^{2+} and Cd^{2+} discriminable fluorescent sensor.

2. Results and discussion

2.1 Design and synthesis of sensor BMD

To date a number of conventional sensing mechanisms, such as photoinduced electron transfer (PET),[1a] intramolecular charge transfer (ICT),[1a] electronic energy transfer (EET),[1a] fluorescence resonance energy transfer (FRET),[13] and excimer formation,[1a] have been developed and applied to the optical detection of different target species. Recently, a new sensing mechanism based on the modulation of excited-state intramolecular proton transfer (ESIPT)[14] has been explored in ion detection; the commonly used ESIPT fluorophores are focused on 2-(2′-hydroxyphenyl)benzoxazole and 2-(2′-hydroxyphenyl)-benzothiazole, and they are generally applied to anion recognition through inhibition[15] or turn on[16] of the ESIPT process; only very few examples based on the modulation of ESIPT have been documented for metal cation sensing.[17] Although the ESIPT feature of 2-(2′-aminophenyl)benzimidazole (2-APBI) and its derivatives has been well investigated for many years, only one study on 2-(2′-benzenesulfonamidophenyl)benzimidazole derivatives as Zn^{2+} sensors based on inhibition of ESIPT has been reported.[17f] Unfortunately, those probes also seriously suffer from the interference of Cd^{2+}. Early studies demonstrated that 2-(2′-acetamidophenyl)benzimidazole displays a more active ESIPT process compared with that of its parent compound 2-APBI,[18] because the introduced electron-withdrawing acetyl group can greatly increase the acidity of 2′-NH, which is favorable to ESIPT. However, metal ion recognition by using of this kind of probe has not been reported so far. One can envision that if the ESIPT process can be inhibited through a metal ion binding process, it is possible to develop a ratiometric probe for the metal ion. Furthermore, if the metal ion in the formed metal-fluorophore complex can be snatched by a certain anion, the inhibited ESIPT will revive, thus resulting in ratiometric recognition of the anion. Based on this idea, we designed and synthesized a new DPA-decorated 2-APBI derivative **BMD** as a promising fluorescent sensor.

The sensor **BMD** was facilely synthesized by reaction of *N*-[2-(1*H*-benzoimidazol-2-yl)-phenyl]-2-chloroacetamide (2) with DPA (Scheme 1). The structure of **BMD** was characterized by ^{1}H NMR, ^{13}C NMR, high resolution mass spectroscopy (HRMS) (see Electronic Supplementary Information†), and single crystal X-ray structural analysis (Fig. 1). The X-ray crystallographic structure clearly indicates that the introduced DPA moiety together with the amide and imino nitrogen atoms can provide coordination sites when **BMD** binds to a certain metal ion. The crystal structure also shows that **BMD** exists in *trans* form (the O and H atoms in the amide group point to opposite sides), and there is an intramolecular hydrogen bond between the amide NH proton and imino nitrogen atom of benzimidazole (N(2)) with a distance of 2.7348 Å; these structural features are favorable to the desired ESIPT process.[18]

2.2 Fluorescence response of BMD to Zn^{2+}

Firstly, the fluorescence spectra of **BMD** in different solvents were examined. As shown in Fig. S1 (ESI†), in aprotic solvents such as cyclohexane, dioxane and acetonitrile, **BMD** displays similar emission spectrum shape with a longer-wavelength emission band at around 513 nm accompanied with a large Stokes shift greater than 180 nm. This longer-wavelength

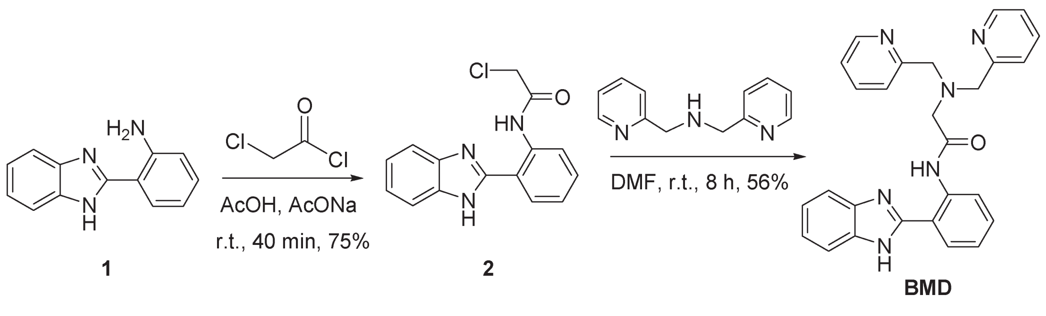

Scheme 1 Synthesis of sensor **BMD**.

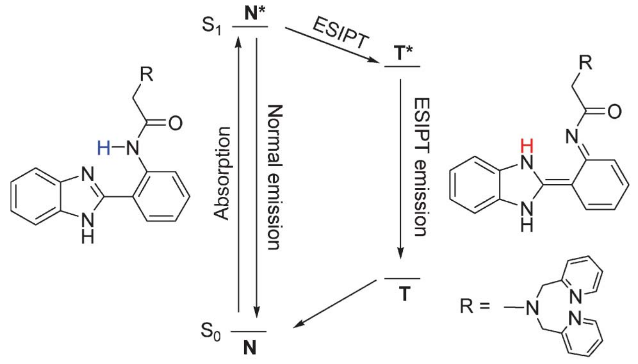

Scheme 2 Emission mechanism for sensor **BMD**.

emission is assigned to the ESIPT fluorescence emission band (tautomer emission). Meanwhile, there are also three adjacent shorter-wavelength emission bands at around 370 nm (normal emission bands). When in protic solvents such as methanol and water, the longer-wavelength emission is slightly blue shifted to 503 nm and 499 nm, respectively. Interestingly, in neat water solution, the fine structure of normal emission bands fused together and only behaves as a single smooth emission band centered at 373 nm. These observations are very similar to the ESIPT phenomena of 2-(2′-acetamidophenyl)benzimidazole[18] and 2-(2′-benzamidophenyl)benzimidazole.[19] The emission mechanism of sensor **BMD** is illustrated in Scheme 2. For the sake of good probe solubility and potential applicability, a cosolvent of CH_3CN/H_2O (2 : 8, v/v) was selected in this study.

Then, the fluorescence response of **BMD** (10 μM) in CH_3CN/H_2O (2 : 8, v/v, pH 7.4) to various metal ions was examined (Fig. 2). Free **BMD** solution exhibits a strong emission band at 502 nm (tautomer emission) and a weak emission band at 367 nm (normal emission) upon being excited at 315 nm. Upon addition of 1.0 equiv. of Zn^{2+}, the emission intensities at 502 nm and 367 nm were greatly decreased, concomitantly a new emission band centered at 424 nm appeared with 78 nm of longer-wavelength emission blue-shift. The addition of 1.0 equiv. Cd^{2+} ions resulted in a 23 nm blue-shift of the longer-wavelength emission from 502 nm to 479 nm. The distinct blue-shifts induced by these two metal ions indicate that Zn^{2+} and Cd^{2+} coordinate with the **BMD** fluorophore in different manners, which elicit intramolecular charge transfer to different extents. Other HTM ions did not induce any significant emission wavelength shift. Among them, Hg^{2+} and Ag^+ caused a slight decrease in fluorescence intensity, and Fe^{2+} and Pb^{2+} led to a moderate quenching effect. However, Cu^{2+}, Co^{2+} and Ni^{2+} ions resulted in almost complete fluorescence quenching owing to their paramagnetic nature. The presence of metal ions including K^+, Na^+, Mg^{2+}, Ca^{2+}, Sr^{2+}, Ba^{2+}, Al^{3+}, Fe^{3+} and Mn^{2+} do not induce noticeable fluorescence spectra changes. These observations reveal that the sensor **BMD** shows specific responses to Zn^{2+} and Cd^{2+} over other metal ions, and **BMD** can clearly discriminate Zn^{2+} from Cd^{2+} by the distinct longer-wavelength emission blue-shift.

The sensing property of **BMD** to Zn^{2+} was further evaluated by fluorescence titration experiment (Fig. 3). The emission intensities at 367 nm and 502 nm of **BMD** solution progressively decreased on incremental increasing the added Zn^{2+} concentration. Meanwhile, the intensity of the newly formed emission band at 424 nm gradually increased. The titration reached saturation when 1.0 equiv. of Zn^{2+} ions was employed, suggesting the formation of a 1 : 1 complex between **BMD** and Zn^{2+}, which was further confirmed by Job's plot (Fig. S2, ESI†). HRMS analysis of the **BMD** solution in the presence of Zn^{2+} exhibited a prominent peak at *m*/*z* 511.1219, which is assignable to the species of $[\mathbf{BMD} + Zn^{2+} - H^+]^+$ (Fig. S3, ESI†). This result presented solid evidence for the 1 : 1 interaction between **BMD** and Zn^{2+}. The well-defined isoemissive points appearing at 379 nm and 458 nm indicate the existence of an equilibrium between free **BMD** and a **BMD**-Zn^{2+} complex. Thus, sensor **BMD** displays a ratiometric response output to Zn^{2+}. Based on the titration profile, the binding constant was evaluated to be $1.63 \times 10^5\ M^{-1}$ (Fig. S4, ESI†) by using the Hill plot method,[20] and the detection limit

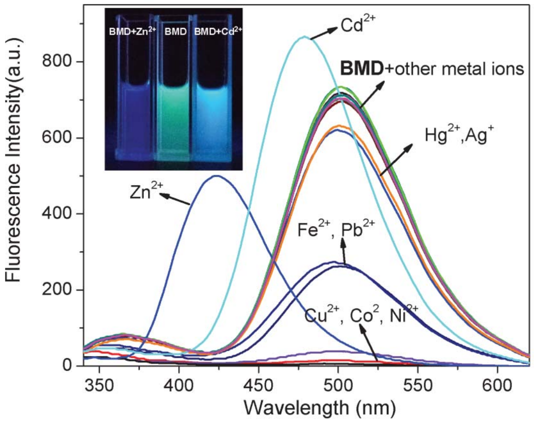

Fig. 2 Fluorescence spectra changes of **BMD** (10 μM) in CH_3CN/H_2O (2 : 8, v/v, HEPES 10 mM, pH 7.4) in the presence of 1.0 equiv. of different metal ions. Inset: The naked eye fluorescence changes of **BMD** before and after addition of Zn^{2+} and Cd^{2+} ions under the portable UV lamp at 254 nm.

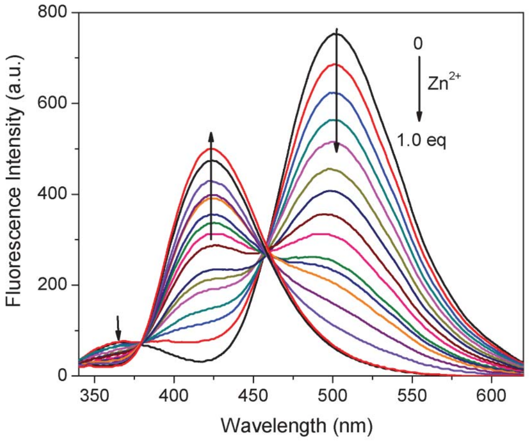

Fig. 3 Fluorescence spectra changes of **BMD** (10 μM) solution upon the addition of different amounts of Zn^{2+}.

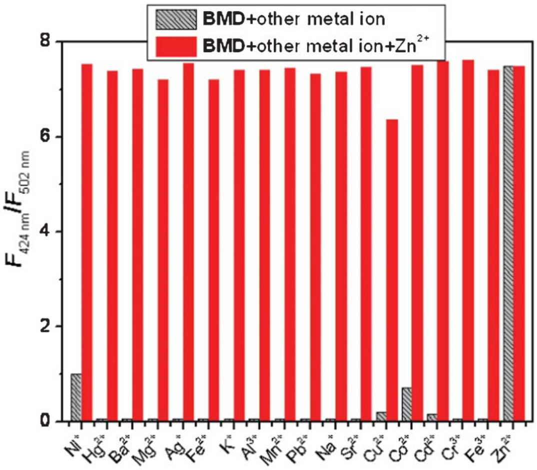

Fig. 4 Changes in the fluorescence intensity ratios (F_{424nm}/F_{502nm}) of **BMD** solution (10 μM) in CH_3CN/H_2O (2 : 8, v/v, HEPES 10 mM, pH 7.4). The gray bars represent the intensity ratio F_{424nm}/F_{502nm} of **BMD** solution in the presence of 1.0 equiv. of different metal ions. The red bands represent the intensity ratio (F_{424nm}/F_{502nm}) of **BMD** for 1.0 equiv. of Zn^{2+} in the presence of different metal ions.

of **BMD** to Zn^{2+} was evaluated to be 6.21×10^{-7} M (Fig. S5, ESI†). Fluorescence changes of the **BMD** solution with 1.0 equiv. of Zn^{2+} at different pH values were examined. The results demonstrate that the intensity ratios (F_{424nm}/F_{502nm}) are almost stable between pH 6 and 9 (Fig. S6, ESI†). Both strong acidic and basic conditions can induce a decrease in the intensity ratio (F_{424nm}/F_{502nm}). These results indicate the potential practical applicability of **BMD** for Zn^{2+} detection in real water samples.

To further confirm the high selectivity of **BMD** to Zn^{2+}, fluorescence competition experiments were then conducted (Fig. 4). The emission intensity ratios (F_{424nm}/F_{502nm}) of **BMD** solution in the presence of miscellaneous metal ions did not show significant changes. Upon further addition of Zn^{2+} to metal ion containing **BMD** solution, the ratios of F_{424nm}/F_{502nm} significantly increased. These results further corroborate the high selectivity of **BMD** to Zn^{2+} without significant interference from other metal ions.

To get further insight into the binding mode of **BMD** and Zn^{2+}, the ^{1}H NMR spectrum of **BMD** in DMSO-d$_6$ in the presence of 1.0 equiv. of Zn^{2+} was determined and the result was shown in Fig. 5. The amide NH (H$_a$) signal appeared at 13.26 ppm in free **BMD** (Fig. 5a), which disappeared upon the addition of 1.0 equiv. of Zn^{2+} (Fig. 5b). However, the imidazole NH (H$_b$) signal at 13.16 ppm became broadened with a small downfield shift. The Zn^{2+}-induced disappearance of the amide NH proton may be attributed to the transformation of the amide group to imidic acid upon binding with Zn^{2+},[7i,8g,21] which also implies that the negatively charged oxygen atom in deprotonated imidic acid may coordinate with Zn^{2+}.[22] This Zn^{2+} binding event suppressed the ESIPT process of **BMD** and led to the ratiometric fluorescence changes. The signal appearing at 8.77 ppm (Fig. 5 a) can be assigned to the H$_f$ (C(12) proton, see Fig. 1) due to the existence of hydrogen bonding between H$_f$ and the amide O atom (2.8503 Å). Upon addition of Zn^{2+} this signal shifted upfield to about 8.0 ppm (Fig. 5b), indicating the coordination of the amide O atom with Zn^{2+}, which weakened the hydrogen bonding. The signal of protons H$_e$ neighbouring pyridine N atom at 8.47 ppm are shifted downfield to 8.68 ppm upon addition of Zn^{2+}. In addition, the methylene protons (H$_c$) adjacent to the amide group signal at 3.44 ppm (Fig. 5a) shifted downfield to 4.12 ppm after the addition of Zn^{2+} (Fig. 5b). Meanwhile, the singlet peak of the methylene protons (H$_d$) in the DPA moiety at 4.0 ppm (Fig. 5a) is shifted downfield and divided into two nonequivalent groups (appearing at 4.64 ppm and 4.42 ppm, respectively) with a large coupling constant of 16 Hz (Fig. 5b), which indicates that the free rotation of σ bonds in DPA is suppressed after coordination with Zn^{2+}. Thus the ^{1}H NMR studies demonstrate that **BMD** binds with Zn^{2+} through an imidic acid form, and the amide oxygen and DPA nitrogen atoms are involved in coordination with Zn^{2+}. The proposed binding mode of **BMD** with Zn^{2+} is depicted in Fig. 5.

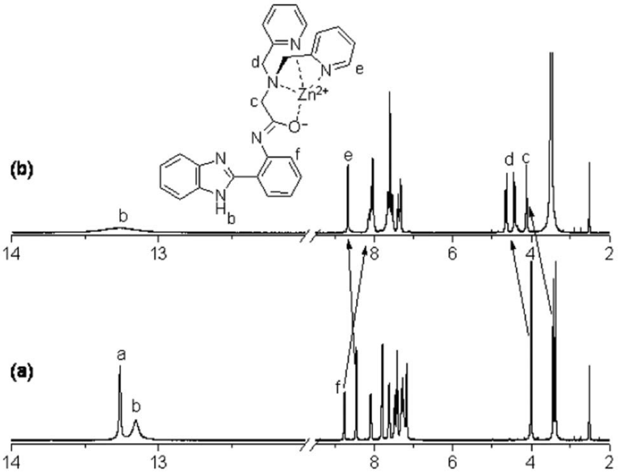

Fig. 5 ^{1}H NMR spectrum of **BMD** in DMSO-d$_6$ without (a) and with (b) 1.0 equiv. of Zn^{2+} and the proposed binding mode of **BMD** with Zn^{2+}.

Similarly, we explored the fluorescence titration of the **BMD** solution with different concentrations of Cd^{2+} ions (Fig. 6). When the Cd^{2+}/**BMD** ratio is smaller than 0.6, the fluorescence intensity was enhanced gradually and blue-shifted from 502 nm to 486 nm (Fig. 6a). Upon further addition of Cd^{2+} ions (0.7–1.5 eq.), however, the emission intensity at 486 nm gradually decreased and further blue-shifted to 479 nm (Fig. 6b). These results indicate the formation of two different metal complexes between **BMD** and Cd^{2+}, the metal/ligand ratios of which may 1 : 2 and 1 : 1, respectively.[23] This speculation was confirmed by HRMS analysis of **BMD** solution in the presence of 0.5 equiv. and 1.0 equiv. of Cd^{2+} ions, respectively (Fig. S7 and S8, ESI†). These complicated binding modes retarded the quantitative detection of Cd^{2+} with **BMD**.

2.3 Fluorescence recognition of BMD-Zn^{2+} for sulfide

Considering the high affinity of sulfide to Zn^{2+}, the *in situ* formed **BMD**-Zn^{2+} complex (1 : 1 mixing of **BMD** and Zn^{2+}) was explored as a promising S^{2-} sensor. Fig. 7 shows the fluorescence spectra changes of **BMD**-Zn^{2+} solution (10 μM)

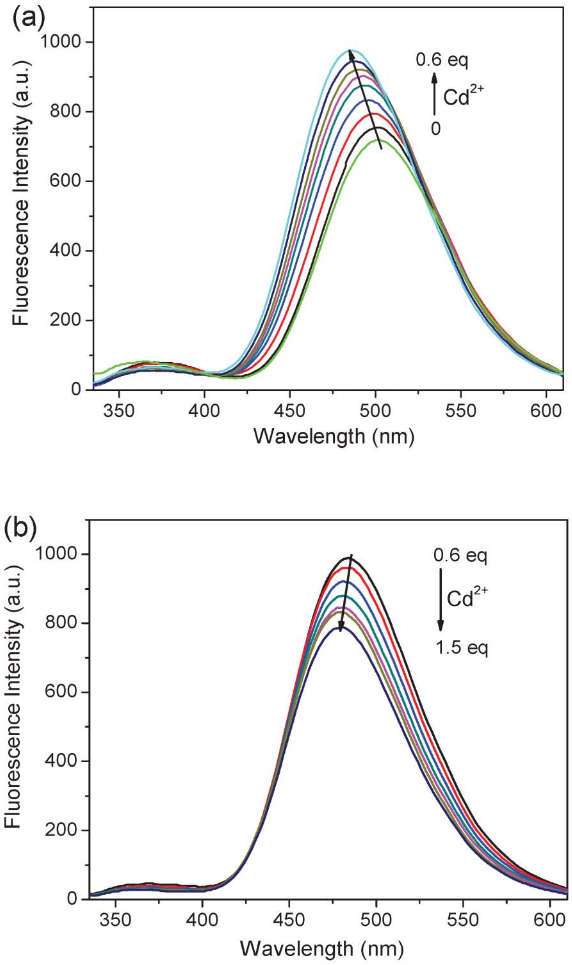

Fig. 6 Fluorescence spectra changes of **BMD** solution (10 μM) upon addition of 0–0.6 equiv. (a) and 0.6–1.5 equiv. (b) of Cd^{2+} in CH_3CN/H_2O (2 : 8, v/v, HEPES 10 mM, pH 7.4).

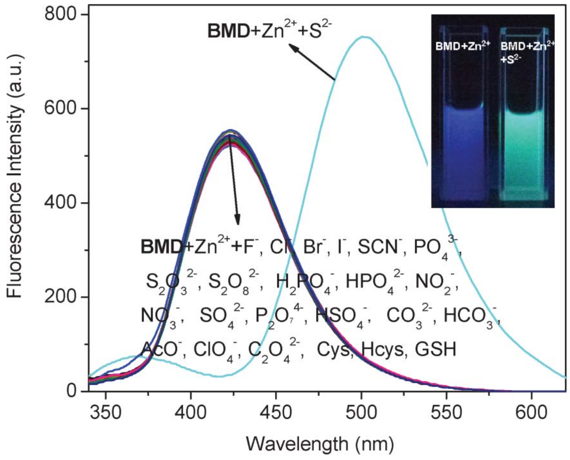

Fig. 7 Fluorescence spectra changes of **BMD**-Zn^{2+} (10 μM) in CH_3CN/H_2O (2 : 8, v/v, HEPES 10 mM, pH 7.4) in the presence of 20 equiv. of different anions and thiol-containing amino acids. Inset: The naked eye fluorescence changes of **BMD**-Zn^{2+} before and after addition of S^{2-} ions under the portable UV lamp at 254 nm.

in the presence of 20 equiv. of different anions including F^-, Cl^-, Br^-, I^-, CN^-, SCN^-, PO_4^{3-}, $S_2O_3^{2-}$, $S_2O_8^{2-}$, $H_2PO_4^-$, HPO_4^{2-}, NO_2^-, NO_3^-, SO_4^{2-}, $P_2O_7^{4-}$, HSO_4^-, CO_3^{2-}, HCO_3^-, AcO^-, ClO_4^-, $C_2O_4^{2-}$, and some thiol-containing amino acids such as L-cysteine (L-Cys), L-homocysteine (L-Hcys) and reduced glutathion (GSH). Obviously, only the addition of S^{2-} anions resulted in significant fluorescence spectrum changes. The emission at 424 nm was greatly quenched, meanwhile two new emission bands at 367 nm and 502 nm were developed. Other anions and thiol-containing amino acids induced almost negligible fluorescence changes. These results demonstrate that the sensor **BMD**-Zn^{2+} has an excellent selectivity toward the S^{2-} ion.

Fluorescence titration experiments were subsequently conducted to examine the sensing property of **BMD**-Zn^{2+} to S^{2-} (Fig. 8). Upon gradually increasing the S^{2-} concentration (0–20 equiv.), the emission band at 424 nm progressively decreased, and simultaneously the emission peak at 502 nm was gradually enhanced. When 20 equiv. of S^{2-} anions was employed, the fluorescence spectrum became stable and was restored to the original emission pattern of free **BMD**. The almost complete fluorescence emission recovery of **BMD**-Zn^{2+} to the original state of free **BMD** strongly indicates an S^{2-}-induced Zn^{2+} removal process. Solid evidence for this S^{2-}-induced Zn^{2+} sequestering came from the HRMS spectrum of **BMD**-Zn^{2+} solution in the presence of S^{2-} anions (Fig. S9, ESI†). The peak for the **BMD**-Zn^{2+} complex disappeared and a peak at m/z 471.1914 assignable to $[\mathbf{BMD} + Na^+]^+$ was observed, indicative of the S^{2-}-induced Zn^{2+} sequestering from **BMD**-Zn^{2+}, which is responsible for the ESIPT restoration of **BMD**. The detection limit of **BMD**-Zn^{2+} to S^{2-} was evaluated to be 3.46×10^{-6} M (Fig. S10, ESI†).

The excellent selectivity of **BMD**-Zn^{2+} to S^{2-} was further validated by competition experiments (Fig. 9). In the absence of S^{2-}, the emission intensity ratios (F_{424nm}/F_{502nm}) of **BMD**-Zn^{2+} solution upon the addition different anions and thiol-containing amino acids (20 equiv. of each) were similar and scarcely fluctuated. Upon further addition of 20 equiv. of S^{2-} to the solution containing other tested species, the emission

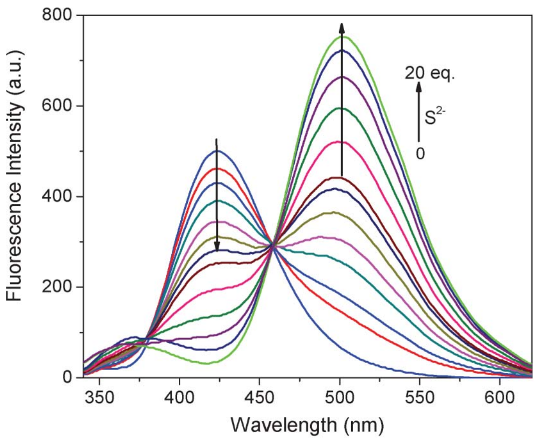

Fig. 8 Fluorescence spectra changes of **BMD**-Zn^{2+} solution (10 μM) upon addition of different amounts of S^{2-}.

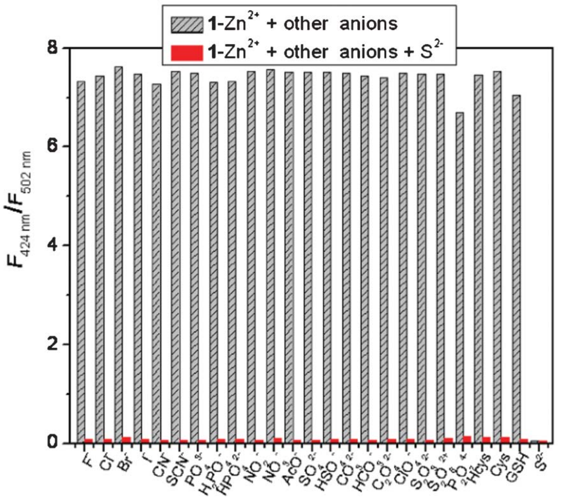

Fig. 9 Changes of intensity ratios (F_{424nm}/F_{502nm}) of **BMD**-Zn^{2+} solution (10 μM) in CH_3CN/H_2O (2 : 8, v/v, HEPES 10 mM, pH 7.4). The gray bars represent the intensity ratio (F_{424nm}/F_{502nm}) of **BMD**-Zn^{2+} solution in the presence of 20 equiv. of different anions. The red bards represent the intensity ratio (F_{424nm}/F_{502nm}) of **BMD**-Zn^{2+} to S^{2-} in the presence of others anions.

ratios of the tested solutions were all greatly decreased and reached the similar level. These facts further demonstrate the high selectivity of **BMD**-Zn^{2+} to S^{2-}.

To evaluate the practical applicability, the potential utilities of **BMD** were checked by proof-of-concept experiments.[24] Tap, lake and river water were collected from laboratory, Tinglin lake (in Bohai University), and Xiaoling river (Linghe district, Jinzhou), respectively. Different concentrations of Zn^{2+} or S^{2-} were spiked into these samples before **BMD** (10 μM) was added. The intensity ratios (F_{424nm}/F_{502nm}) were proportional to the concentrations of Zn^{2+} in the range of 0 to 6 μM (Fig. S11, ESI†). Similarly, when this method was applied to sulfide detection with **BMD**-Zn^{2+} system, good linear dependence of fluorescence intensity on S^{2-} concentration were also obtained in the range of 10 to 50 μM (Fig. S12, ESI†). Therefore, the presented sensors **BMD** and **BMD**-Zn^{2+} could be used for trace Zn^{2+} and S^{2-} analyses in these three complicated environmental systems, respectively.

3. Conclusions

In conclusion, we have developed a simple fluorescent sensor, **BMD**. It behaves a ratiometric response to Zn^{2+} with good discrimination from Cd^{2+} and other metal ions. The *in situ* formed **BMD**-Zn^{2+} shows a ratiometric response to sulfide anion with excellent selectivity and sensitivity. Proof-of-concept experiments also provided the potential applicability of **BMD** in real water sample analysis. Thus, **BMD** can be used as a fluorescent sensor for sequential detection of Zn^{2+} and S^{2-} in water.

4. Experimental section

4.1 Materials and instruments

Unless otherwise stated, solvents and reagents were of analytical grade from commercial suppliers and were used without further purification. Compound 2 was prepared by the literature method.[25] ^1H NMR and ^{13}C NMR spectra were recorded on Agilent 400-MR spectrometer. Chemical shifts (δ) were expressed in ppm and coupling constants (*J*) in Hertz. HRMS was measured on an Agilent 1200 time-of-flight mass spectrometer (Bruker, micrOTOF-Q). Fluorescence measurements were performed on a Sanco 970-CRT spectrofluorometer (Shanghai, China). The pH measurements were made with a Model PHS-25B meter (Shanghai, China).

4.2 Synthesis of sensor BMD

To a solution of *N*-[2-(1*H*-benzoimidazol-2-yl)-phenyl]-2-chloroacetamide (2) (0.51 g, 1.8 mmol) in 8 mL of DMF, DPA (1.39 g, 7.2 mmol) was added. The reaction mixture was stirred at room temperature for 8 h, and then poured into 150 mL of distilled water and adjusted to pH 7. The resulting precipitates was collected by filtration and washed with H_2O, dried and recrystallized from acetonitrile to give 0.45 g of **BMD** as brown solid. Yield: 56%. M.p. 177–179 °C. ^1H NMR (400 MHz, DMSO-d_6) δ 13.26 (s, 1H), 13.16 (s, 1H), 8.77 (d, *J* = 8.8 Hz, 1H), 8.47 (d, *J* = 4.0 Hz, 2H), 8.09 (d, *J* = 7.6 Hz, 1H), 7.81 (d, *J* = 8.0 Hz, 2H), 7.63 (d, *J* = 6.4 Hz, 2H), 7.49 (t, *J* = 8.0 Hz, 1H), 7.43 (t, *J* = 8.0 Hz, 2H), 7.37–7.22 (m, 3H), 7.20–7.17 (m, 2H), 4.00 (s, 4H), 3.44 (s, 2H). ^{13}C NMR (100 MHz, DMSO-d_6). δ 170.47, 158.25, 150.95, 149.24, 138.09, 136.74, 130.89, 128.22, 123.51, 123.43, 122.74, 120.74, 116.90, 60.53, 58.79. HRMS (ESI+) calcd for $C_{27}H_{24}N_6ONa$ $[M + Na]^+$, 471.1909; Found 471.1908.

4.3 General procedure for spectroscopic analysis

Doubly distilled water was used for all experiments. Compound **BMD** was dissolved in CH_3CN/H_2O (2 : 8, v/v, HEPES 10 mM, pH 7.4) to afford the test solution (10 μM). Titration experiments were carried out in 10-mm quartz cuvettes at 25 °C. Metal ions (as chloride or nitrate salts, 10 mM) and anions (as sodium salts, 10 mM and 100 mM) in CH_3CN/H_2O (2 : 8, v/v, HEPES 10 mM, pH 7.4) were added to the host solution and used for the titration experiment.

BMD-Zn^{2+} solution for sulfide anion detection was prepared by addition of 1.0 equiv. of Zn^{2+} to compound **BMD** solution (10 μM) in CH_3CN/H_2O (2 : 8, v/v, HEPES 10 mM, pH 7.4).

Acknowledgements

We are grateful to the NSFC (No. 21176029), the Natural Science Foundation of Liaoning Province (No. 20102004) and the Program for Liaoning Excellent Talents in University (No. LJQ2012096) for financial support.

Notes and References

1 (*a*) A. P. de Silva, H. Q. N. Gunaratne, T. Gunnlaugsson, A. J. M. Huxley, C. P. McCoy, J. T. Rademacher and T. E. Rice,

Chem. Rev., 1997, **97**, 1515–1566; (*b*) T. Gunnlaugsson, M. Glynn, G. M. Tocci, P. E. Kruger and F. M. Pfeffer, *Coord. Chem. Rev.*, 2006, **250**, 3094–3117; (*c*) B. Valeur and I. Leray, *Coord. Chem. Rev.*, 2000, **205**, 3–40; (*d*) J. Du, M. Hu, J. Fan and X. Peng, *Chem. Soc. Rev.*, 2012, **41**, 4511–4535; (*e*) M. E. Jun, B. Roy and K. H. Ahn, *Chem. Commun.*, 2011, **47**, 7583–7601; (*f*) P. D. Beer and P. A. Gale, *Angew. Chem., Int. Ed.*, 2001, **40**, 486–516; (*g*) X. Lou, D. Ou, Q. Li and Z. Li, *Chem. Commun.*, 2012, **48**, 8462–8477; (*h*) M. Wenzel, J. R. Hiscock and P. A. Gale, *Chem. Soc. Rev.*, 2012, **41**, 480–520.

2 (*a*) J. M. Berg and Y. Shi, *Science*, 1996, **271**, 1081–1085; (*b*) S. C. Burdette and S. J. Lippard, *Proc. Natl. Acad. Sci. U. S. A.*, 2003, **100**, 3605–3610; (*c*) P. J. Fraker and L. E. King, *Annu. Rev. Nutr.*, 2004, **24**, 277–298; (*d*) W. J. Bettger and B. L. O'Dell, *J. Nutr. Biochem.*, 1993, **4**, 194–207.

3 (*a*) C. F. Walker and R. E. Black, *Annu. Rev. Nutr.*, 2004, **24**, 255–275; (*b*) D. W. Choi and J. Y. Koh, *Annu. Rev. Neurosci.*, 1998, **21**, 347–375; (*c*) J. H. Weiss, S. L. Sensi and J. Y. Koh, *Trends Pharmacol. Sci.*, 2000, **21**, 395–401.

4 Z. Xu, J. Yoon and D. R. Spring, *Chem. Soc. Rev.*, 2010, **39**, 1996–2006.

5 (*a*) Y. Kawanishi, K. Kikuchi, H. Takakusa, S. Mizukami, Y. Urano, T. Higuchi and T. Nagano, *Angew. Chem., Int. Ed.*, 2000, **39**, 3438–3440; (*b*) C. C. Woodroofe and S. J. Lippard, *J. Am. Chem. Soc.*, 2003, **125**, 11458–11459; (*c*) Z. Liu, C. Zhang, Y. Li, Z. Wu, F. Qian, X. Yang, W. He, X. Gao and Z. Guo, *Org. Lett.*, 2009, **11**, 795–798.

6 (*a*) M. Taki, J. L. Wolford and T. V. O'Halloran, *J. Am. Chem. Soc.*, 2004, **126**, 712–713; (*b*) H.-H. Wang, Q. Gan, X.-J. Wang, L. Xue, S.-H. Liu and H. Jiang, *Org. Lett.*, 2007, **9**, 4995–4998; (*c*) D. Du, M. Wang, J. Cai and A. Zhang, *Sens. Actuators, B*, 2010, **146**, 337–341; (*d*) E. Tamanini, A. Katewa, L. M. Sedger, M. H. Todd and M. Watkinson, *Inorg. Chem.*, 2009, **48**, 319–324.

7 (*a*) K. Hanaoka, K. Kikuchi, H. Kojima, Y. Urano and T. Nagano, *Angew. Chem., Int. Ed.*, 2003, **42**, 2996–2999; (*b*) W. Liu, L. Xu, R. Sheng, P. Wang, H. Li and S. Wu, *Org. Lett.*, 2007, **9**, 3829–3832; (*c*) M. Taki, M. Desaki, A. Ojida, S. Iyoshi, T. Hirayama, I. Hamachi and Y. Yamamoto, *J. Am. Chem. Soc.*, 2008, **130**, 12564–12565; (*d*) F. Qian, C. Zhang, Y. Zhang, W. He, X. Gao, P. Hu and Z. Guo, *J. Am. Chem. Soc.*, 2009, **131**, 1460–1468; (*e*) E. Tomat, E. M. Nolan, J. Jaworski and S. J. Lippard, *J. Am. Chem. Soc.*, 2008, **130**, 15776–15777; (*f*) L. Xue, C. Liu and H. Jiang, *Chem. Commun.*, 2009, 1061–1063; (*g*) T. Cheng, Y. Xu, S. Zhang, W. Zhu, X. Qian and L. Duan, *J. Am. Chem. Soc.*, 2008, **130**, 16160–16161; (*h*) G. Masanta, C. S. Lim, H. J. Kim, J. H. Han, H. M. Kim and B. R. Cho, *J. Am. Chem. Soc.*, 2011, **133**, 5698–5700; (*i*) Z. Xu, X. Liu, J. Pan and D. R. Spring, *Chem. Commun.*, 2012, **48**, 4764–4766; (*j*) M.-M. Yu, Z.-X. Li, L.-H. Wei, D.-H. Wei and M.-S. Tang, *Org. Lett.*, 2008, **10**, 5115–5118; (*k*) Y. Zhou, Z.-X. Li, S.-Q. Zang, Y.-Y. Zhu, H.-Y. Zhang, H.-W. Hou and T. C. W. Mak, *Org. Lett.*, 2012, **14**, 1214–1217; (*l*) Z. Li, M. Yu, L. Zhang, M. Yu, J. Liu, L. Wei and H. Zhang, *Chem. Commun.*, 2010, **46**, 7169–7171; (*m*) Z. Li, L. Zhang, L. Wang, Y. Guo, L. Cai, M. Yu and L. Wei, *Chem. Commun.*, 2011, **47**, 5798–5800.

8 (*a*) Z.-X. Han, X.-B. Zhang, Z. Li, Y.-J. Gong, X.-Y. Wu, Z. Jin, C.-M. He, L.-X. Jian, J. Zhang and G.-L. Shen, *Anal. Chem.*, 2010, **82**, 3108–3113; (*b*) L. Xue, Q. Liu and H. Jiang, *Org. Lett.*, 2009, **11**, 3454–3457; (*c*) L. Xue, C. Liu and H. Jiang, *Org. Lett.*, 2009, **11**, 1655–1658; (*d*) J. Wang, W. Lin and W. Li, *Chem.–Eur. J.*, 2012, **18**, 13629–13632; (*e*) X. Zhou, P. Li, Z. Shi, X. Tang, C. Chen and W. Liu, *Inorg. Chem.*, 2012, **51**, 9226–9231; (*f*) C. Lu, Z. Xu, J. Cui, R. Zhang and X. Qian, *J. Org. Chem.*, 2007, **72**, 3554–3557; (*g*) Z. Xu, K.-H. Baek, H. N. Kim, J. Cui, X. Qian, D. R. Spring, I. Shin and J. Yoon, *J. Am. Chem. Soc.*, 2010, **132**, 601–610.

9 *Hydrogen Sulfide*, World Health Organization: Geneva, 1981, (EnvironmentalHealth Criteria, No. 19).

10 (*a*) X. Cao, W. Lin and L. He, *Org. Lett.*, 2011, **13**, 4716–4719; (*b*) S. A. Patwardhan and S. M. Abhyankar, *Colourage*, 1988, **35**, 15–18.

11 (*a*) D. Jiménez, R. Martínez-Máñez, F. Sancenón, J. V. Ros-Lis, A. Benito and J. Soto, *J. Am. Chem. Soc.*, 2003, **125**, 9000–9001; (*b*) X. Lou, H. Mu, R. Gong, E. Fu, J. Qin and Z. Li, *Analyst*, 2011, **136**, 684–687; (*c*) L. Zhang, X. Lou, Y. Yu, J. Qin and Z. Li, *Macromolecules*, 2011, **44**, 5186–5193; (*d*) J. Liu, J. Chen, Z. Fang and L. Zeng, *Analyst*, 2012, **137**, 5502–5505; (*e*) M.-Q. Wang, K. Li, J.-T. Hou, M.-Y. Wu, Z. Huang and X.-Q. Yu, *J. Org. Chem.*, 2012, **77**, 8350–8354; (*f*) R. Zhang, X. Yu, Y. Yin, Z. Ye, G. Wang and J. Yuan, *Anal. Chim. Acta*, 2011, **691**, 83–88; (*g*) Y. Qian, J. Karpus, O. Kabil, S.-Y. Zhang, H.-L. Zhu, R. Banerjee, J. Zhao and C. He, *Nat. Commun.*, 2011, **2**, 495; (*h*) J. Zhang, X. Xu and X. Yang, *Analyst*, 2012, **137**, 1556–1558.

12 (*a*) M. G. Choi, S. Cha, H. Lee, H. L. Jeon and S.-K. Chang, *Chem. Commun.*, 2009, 7390–7392; (*b*) F. Hou, L. Huang, P. Xi, J. Cheng, X. Zhao, G. Xie, Y. Shi, F. Cheng, X. Yao and D. Bai, *Inorg. Chem.*, 2012, **51**, 2454–2460; (*c*) F. Hou, J. Cheng, P. Xi, F. Chen, L. Huang, G. Xie, Y. Shi, H. Liu, D. Bai and Z. Zeng, *Dalton Trans.*, 2012, **41**, 5799–5804; (*d*) X. Gu, C. Liu, Y.-C. Zhu and Y.-Z. Zhu, *Tetrahedron Lett.*, 2011, **52**, 5000–5003.

13 K. E. Sapsford, L. Berti and I. L. Medintz, *Angew. Chem., Int. Ed.*, 2006, **45**, 4562–4589.

14 (*a*) J. Wu, W. Liu, J. Ge, H. Zhang and P. Wang, *Chem. Soc. Rev.*, 2011, **40**, 3483–3495; (*b*) J. Zhao, S. Ji, Y. Chen, H. Guo and P. Yang, *Phys. Chem. Chem. Phys.*, 2012, **14**, 8803–8817.

15 (*a*) Y.-G. Zhao, B.-G. Zhang, C.-Y. Duan, Z.-H. Lin and Q.-J. Meng, *New J. Chem.*, 2006, **30**, 1207–1213; (*b*) Y. Wu, X. Peng, J. Fan, S. Gao, M. Tian, J. Zhao and S. Sun, *J. Org. Chem.*, 2007, **72**, 62–70; (*c*) Q. Chu, D. A. Medvetz and Y. Pang, *Chem. Mater.*, 2007, **19**, 6421–6429; (*d*) A. Helal, N. T. T. Thao, S. W. Lee and H.-S. Kim, *J. Inclusion Phenom. Macrocyclic Chem.*, 2009, **66**, 87–94; (*e*) H. S. Jung, H. J. Kim, J. Vicens and J. S. Kim, *Tetrahedron Lett.*, 2009, **50**, 983–987.

16 (*a*) S. Chen, P. Hou, J. Wang and X. Song, *RSC Adv.*, 2012, **2**, 10869–10873; (*b*) X.-F. Yang, H. Qi, L. Wang, Z. Su and G. Wang, *Talanta*, 2009, **80**, 92–97; (*c*) W.-H. Chen, Y. Xing and Y. Pang, *Org. Lett.*, 2011, **13**, 1362–1365; (*d*) R. Hu, J. Feng, D. Hu, S. Wang, S. Li, Y. Li and G. Yang, *Angew. Chem., Int. Ed.*, 2010, **49**, 4915–4918.

17 (*a*) D. Udhayakumari, S. Saravanamoorthy, M. Ashok and S. Velmathi, *Tetrahedron Lett.*, 2011, **52**, 4631–4635; (*b*) D. Y. Han, J. M. Kim, J. Kim, H. S. Jung, Y. H. Lee, J. F. Zhang and J. S. Kim, *Tetrahedron Lett.*, 2010, **51**, 1947–1951; (*c*) J. Jayabharathi, V. Thanikachalam, N. Srinivasan, K. Jayamorthy and M. V. Perumal, *J. Fluoresc.*, 2011, **21**, 1813–1823; (*d*) K.-C. Wu, Y.-S. Lin, Y.-S. Yeh, C.-Y. Chen, M.

O. Ahmed, P.-T. Chou and Y.-S. Hon, *Tetrahedron*, 2004, **60**, 11861–11868; (*e*) Y. Xu and Y. Pang, *Chem. Commun.*, 2010, **46**, 4070–4072; (*f*) M. M. Henary, Y. Wu and C. J. Fahrni, *Chem.–Eur. J.*, 2004, **10**, 3015–3025.

18 S. Santra, G. Krishnamoorthy and S. K. Dogra, *J. Phys. Chem. A*, 2000, **104**, 476–482.

19 S. Santra, G. Krishnamoorthy and S. K. Dogra, *Chem. Phys. Lett.*, 1999, **311**, 55–61.

20 X. Peng, J. Du, J. Fan, J. Wang, Y. Wu, J. Zhao, S. Sun and T. Xu, *J. Am. Chem. Soc.*, 2007, **129**, 1500–1501.

21 H. G. Lee, J. H. Lee, S. P. Jang, H. M. Park, S.-J. Kim, Y. Kim, C. Kim and R. G. Harrison, *Tetrahedron*, 2011, **67**, 8073–8078.

22 S. Sumiya, Y. Shiraishi and T. Hirai, *J. Phys. Chem. A*, 2013, **117**, 1474–1482.

23 L. J. Liang, X. J. Zhao and C. Z. Huang, *Analyst*, 2012, **137**, 953–958.

24 (*a*) H. Li, J. Fan, F. Song, H. Zhu, J. Du, S. Sun and X. Peng, *Chem.–Eur. J.*, 2010, **16**, 12349–12356; (*b*) H. Zhu, J. Fan, J. Lu, M. Hu, J. Cao, J. Wang, H. Li, X. Liu and X. Peng, *Talanta*, 2012, **93**, 55–61.

25 E. A. Lyakhova, Y. A. Gusyeva, J. V. Nekhoroshkova, L. M. Shafran and S. A. Lyakhov, *Eur. J. Med. Chem.*, 2009, **44**, 3305–3312.